International Journal of Thermophysics, Vol. 27, No. 1, January 2006 (© 2006)
DOI: 10.1007/s10765-006-0013-x

The Viscosity of Organic Liquid Mixtures[1]

C. W. Len,[2] J. P. M. Trusler,[2] V. Vesovic,[3] and W. A. Wakeham[4,5]

The paper reports measurements of the viscosity and density of two heavy hydrocarbon mixtures, Dutrex and Arab Light Flashed Distillate (ALFD), and of their mixtures with hydrogen. The measurements have been carried out with a vibrating-wire device over a range of temperatures from 399 to 547 K and at pressures up to 20 MPa. Measurements have also been carried out on systems in which hydrogen at different concentrations has been dissolved in the liquids. The measurements have an estimated uncertainty of ±5% for viscosity and ±2% for density and represent the first results on these prototypical heavy hydrocarbons. The results reveal that the addition of hydrogen reduces both the density and viscosity of the original hydrocarbon mixture at a particular temperature and pressure.

KEY WORDS: density; hydrogen; mixture; vibrating-wire viscometer; viscosity; wax.

1. INTRODUCTION

Heavy hydrocarbon mixtures that originate from petroleum reservoirs are becoming increasingly important in the petroleum industry. The progressive depletion of easily accessible oil reservoirs has led to advances in extraction technology that allow the recovery of these heavier oils that had previously been left behind. Given that the extraction process and the

---

[1] Paper presented at the Seventh Asian Thermophysical Properties Conference, August 23–28, 2004, Hefei and Huangshan, Anhui, P. R. China.

[2] Department of Chemical Engineering, Imperial College, London SW7 2AZ, United Kingdom.

[3] Department of Earth Science and Engineering, Imperial College, London SW7 2AZ, United Kingdom.

[4] University of Southampton, Highfield, Southampton SO17 1BJ, United Kingdom.

[5] To whom correspondence should be addressed. E-mail: vice-chancellor@soton.ac.uk

industrial use of these fluids are very much influenced by their physical properties, there is considerable interest in the viscosity of one or two prototypical mixtures and of ways of estimating the properties of such mixtures. Very few data on the thermophysical properties of these fluids exist, and estimation methods have therefore yet to be tested for them. The present work is devoted to the design and construction of an instrument for the simultaneous measurement of the viscosity and density of these fluids over a range of temperatures and pressures encountered in reservoirs and its application to the measurement of the viscosity of two model fluids, Dutrex and Arab Light Flash Distillate (ALFD). The viscosity of mixtures with hydrogen is also reported. A vibrating-wire device has been employed for these measurements because it allows simultaneous measurements of viscosity and density in an instrument involving essentially no bulk fluid motion yet capable of high precision at combined high temperatures and pressures. Both hydrocarbon fluids were provided by Shell International. Dutrex is an oil comprising mainly aromatic compounds, while ALFD is a petroleum refinery stream with a boiling range of 640 to 810 K. Selected physiochemical properties of these hydrocarbons, based on information provided by the supplier, are given in Table I.

2. EXPERIMENTAL

The basic principles of vibrating-wire viscometers have been known for some time, but the most complete summaries of the theory of the devices for the measurement of the viscosity and density of fluids have been given by Retsina et al. [1, 2] and Padua et al. [3]. The theory provides a complete description of the instrument and thereby a means of

Table I. Physiochemical Properties of the Hydrocarbons Studied

Property	Value Dutrex	Property	Value ALFD
Melting temperature (°C)	18	Melting temperature (°C)	10
Refractive index at 20°C	1.565	Refractive index at 20°C	1.557
Molecular weight ($g\cdot mol^{-1}$)	400	Molecular weight ($g\cdot mol^{-1}$)	–
Aromatics (mass%)	74.3	Carbon (mass%)	85
Resins (mass%)	10.0	Hydrogen (mass%)	12
Saturates (mass%)	15.7	Oxygen (mass%)	0.3
Carbon (CA%)	40	Carbon (CA%)	12
Carbon (CN%)	34	Carbon (CN%)	55
Carbon (CP%)	26	Carbon (CP%)	33

optimizing designs of instrument to yield specific precisions for prescribed ranges of fluid viscosity and density. In the present application, where we seek to determine the density and viscosity of the fluid simultaneously, we have selected a vibrating-wire configuration in which the wire is tensioned by a suspended weight and have observed the transverse oscillations of the wire in continuous, driven oscillations. In this mode the density of the fluid is determined largely from the change in resonant frequency of the wire oscillations in the liquid from that in *vacuo*, while the viscosity is related to the width of the resonance curve. The instrument employed here has been designed with the principles and constraints set out in Refs. 1–3 in mind but with the specific intent of covering temperature ranges from ambient to 550 K at pressures up to 20 MPa in potentially reactive hydrocarbon mixtures.

Figure 1 illustrates the vibrating-wire assembly employed in the present work, which is described in greater detail elsewhere [4]. The vibrating-wire assembly is mounted from the top cap of a pressure vessel (1), which has a permanent, hollow, cylindrical fixture (2) made from stainless steel attached to it via three short columns (3). A pair of gold-plated samarium–cobalt magnets (4) is mounted onto a cage that sits on the inside of the cylindrical fixture, providing a field of about 0.35 T between them. The vibrating wire is a 100 μm nominal diameter tungsten wire (5) with a nominal length of 64 mm. The top of the wire is clamped to the inside of the cylindrical fixture and the bottom to an aluminium/stainless steel weight (6) with a mass of about 390 g. There is a 1.5 mm concentric clearance between the side of the weight and the pressure vessel wall.

Clamps are used to hold the vibrating wire at each end. The clamps are made of two halves of a solid stainless steel cylinder, held together by stainless steel bolts (7). The electric circuit for driving the vibrating wire and subsequently detecting the signal is provided by a four-wire configuration that enters the viscometer via a high-pressure feed-through in the 6 mm stainless-steel tube at the top of the viscometer (8). The feed wires are made of copper and had a conductor diameter of 0.45 mm with a thin coat of poly-esterimide insulation. Two of these wires are used to provide the driving signal and are soldered onto a tag (9) at the top of the cylindrical fixture. The return path of the electrical signal generated by the vibrating wire is via a copper ribbon (10), which has one end soldered to a tag screwed to the top of the weight. This copper ribbon transmits the signal to a single copper wire (11), which is connected to another two copper wires (12) that exit the viscometer via the stainless-steel tube (8). There is a slot (13) at the top of the pressure vessel cap for housing a platinum resistance thermometer (PRT) to measure the temperature at which

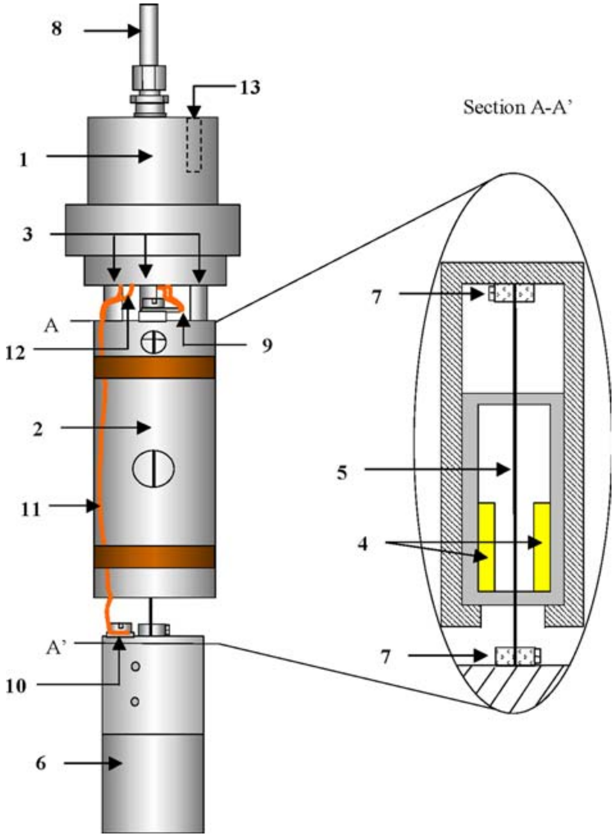

Fig. 1. Vibrating-wire assembly.

viscosity measurements were made. Shaded in Fig. 1 are windings of Kapton tape that secure the copper wire onto the cylindrical fixture.

For measurements up to 500 K this instrument could be used unchanged for a wide range of fluids. Above that temperature, in particular, up to 550 K in the presence of Dutrex, it was necessary to adopt different techniques to provide improved isolation of the copper wires from attack by the reactive fluid. Accordingly, the copper wires were coated with silicone materials and cured at 373 K for two hours followed by enclosing the wires in a PTFE sleeve. The pressure vessel cap itself is, of course, the closure to the pressure vessel containing the test fluid and used a Viton seal up to 500 K and a Kalrez ring up to 550 K. The pressure vessel was

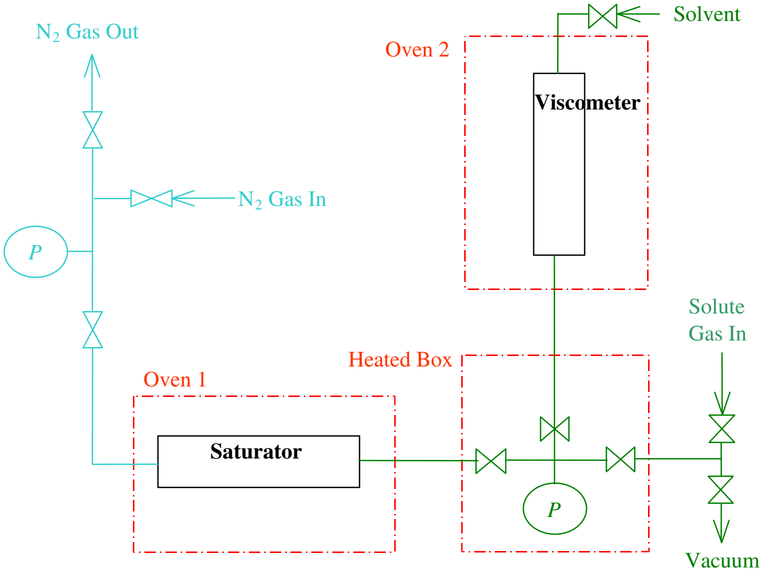

Fig. 2. Connections of the components of the instrument.

suspended from a rigid mount so that it hung vertically. This ensured that the tensioning weight of the vibrating wire was parallel to the axis of the vessel and helped ensure freedom from inadvertent contact between the wall of the pressure vessel and the weight. The viscometer was enclosed within a thermostatically-controlled oven.

The fluids to be studied in this work are solids or very viscous liquids at, or around, ambient conditions of temperature and pressure. Furthermore, it was desired to study the effect of dissolved hydrogen on the viscosity of the fluids. For that reason arrangements had to be made to retain the test fluid at a temperature above ambient (333 K) throughout the entire fluid handling system while also enabling the admixture of gas to the fluid and permitting its mixing with the viscous test fluid. For that reason the pressure vessel in its oven (Oven 2), was connected as shown schematically in Fig. 2 to a saturator, shown in detail in Fig. 3, and a pressure transducer, P, a source of solute gas, a vacuum pump, and a source of pressurizing nitrogen gas. As Fig. 2 shows, the saturator and pressure transducer were each housed in separate furnaces at temperatures such that the test materials were in the liquid state and had a modest viscosity. In addition, all the tubing joining the various components was directly heated and insulated to avoid cold spots anywhere in the system.

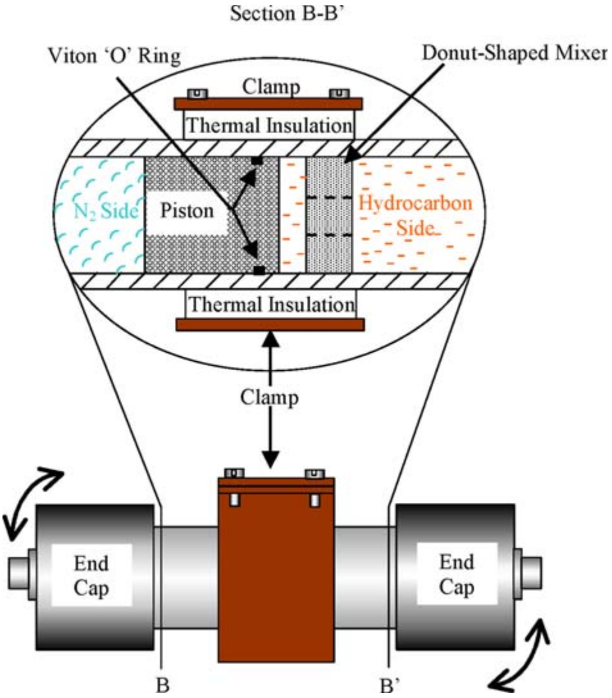

Fig. 3. The saturator.

The full details of this assembly are described elsewhere [4], but here it is sufficient to note that the saturator consists of a free piston mounted in a cylindrical vessel. On one side of the piston the saturator is provided with a high-pressure nitrogen supply which enables the piston to be used as a pump. On the other side the saturator carries a metal annulus which can move freely through the cylinder. The saturator is mounted in a separate oven (Oven 2) in a manner that enables it to be rocked about a horizontal axis perpendicular to the axis of the cylinder. This arrangement allowed the saturator to be partly filled with the test liquid to which gas was added. The subsequent rocking of the saturator stimulated the motion of the annular ring in the right-hand part of the device which promoted mixing of gas and liquid at a rate far higher than was possible by diffusion alone.

When used for measurements on liquids without dissolved gases, the piston of the saturator was withdrawn to the nitrogen gas side and the other side filled with the test liquid. The pressure vessel and pipework were then evacuated and filled with dry nitrogen and the entire assembly heated. Then the nitrogen was displaced by the hydrocarbon liquid by driving the hydrocarbon into the viscometer from the saturator using nitrogen gas. This process ensured that no reaction took place between the hydrocarbon and the oxygen in the air while the viscometer could be definitely said to be full by the emergence of drops of the material from the valve atop the pressure vessel.

When used for measurements with mixtures of the liquid with gas, the test liquid was first poured into the saturator and the system evacuated. Subsequently, the liquid in the saturator and the remainder of the system was heated and the gas was added from its supply. The saturator was then rocked to stimulate mixing for a period of several days. Subsequently the fluid mixture was pumped into the viscometer using the high-pressure nitrogen supply.

By means of carefully weighing the mass of liquid added to the saturator and subsequently determining the mass of hydrogen lost from the hydrogen cylinder in charging the saturator with gas, it was possible to determine the mass fraction of hydrogen dissolved in the liquid phase. The use of different pressures for the supply of hydrogen gas in the cylinder made it possible to secure different concentrations of hydrogen gas within the liquid phase.

In early versions of the vibrating-wire viscometer [5] it was necessary to use special mechanisms to stimulate the forced vibration of the wire in the magnetic field normal to it. In this work we have been able to use much simpler methods. The motion of the wire is stimulated by means of a function generator while a lock-in amplifier is used to directly measure the amplitude and the phase of the signal generated by the oscillating wire. The lock-in amplifier is capable of detecting signals down to the nanovolt level without pre-amplification. The signals recorded for the amplitude and phase of the detected signal are stored digitally for each experimental run for later processing as a record of the velocity resonance curve of the oscillator. These operations are all performed under computer control as is the acquisition of the temperature from the PRT and the pressure from the transducer.

The signal detected at the lock-in amplifier, across the driven vibrating wire, is given by

$$V_{\mathrm{e}} = V_1 + V_2, \tag{1}$$

with $V_1 = IZ$, where Z is the electrical impedance of the stationary wire and I is the driving current; V_2 is the induced signal [4] which, for a driving frequency f, is given by

$$V_2 = \frac{4\,I\,B^2\,f\,L_{\mathrm{m}} \sin\left(\pi\,L_{\mathrm{m}}/2\,L\right)\,\exp\left(i2\pi\,f\,t\right) i}{\pi^3 \rho_{\mathrm{s}} R^2 \left[f_0^2 - f^2\,(1+\beta) + f^2\,(\beta' + 2\Delta_0)\,i\right]} \equiv G\,\Gamma(f)\,\Theta(t), \tag{2}$$

where

$$G = \frac{4IB^2 L_\mathrm{m}}{\pi^3 \rho_\mathrm{s} R^2} \sin\left(\frac{\pi L_\mathrm{m}}{2L}\right), \tag{3}$$

$$\Gamma(f) = \frac{fi}{f_0^2 - f^2(1+\beta) + f^2(\beta' + 2\Delta_0)\, i}, \tag{4}$$

and

$$\Theta(t) = \exp(i 2\pi f t). \tag{5}$$

In practice, the root-mean-square (RMS) voltage generated across the wire is measured using a lock-in amplifier. As a result, the time-dependent term $\Theta(t)$ can be excluded during analysis with the following definition used for practical purposes:

$$V_2 = \frac{Gfi}{f_0^2 - f^2(1+\beta) + f^2(\beta' + 2\Delta_0)\, i}. \tag{6}$$

Here, ρ_s is the density of the wire material, B is the magnetic field intensity, β is the dimensionless added mass of the fluid, β' is the dimensionless drag of the fluid, L_m is the half-length of the magnets, L is the half-length of the wire, and R, is the radius of the vibrating wire. The symbol Δ_0 represents the logarithmic decrement of the oscillations in vacuo. The resonant frequency of the wire, immersed in the fluid, in the absence of viscous drag is denoted by f_0.

Finally,

$$\beta = \rho k / \rho_\mathrm{s}, \tag{7}$$

and

$$\beta' = \rho k' / \rho_\mathrm{s}, \tag{8}$$

where,

$$k = -1 + 2\mathrm{Im}(A), \tag{9}$$

$$k' = 2\mathrm{Re}(A), \tag{10}$$

and

$$A = i\left\{1 + \frac{2K_1\left(\sqrt{i\Omega}\right)}{\sqrt{i\Omega}K_0\left(\sqrt{i\Omega}\right)}\right\}. \tag{11}$$

Here, the Reynolds Number is

$$\Omega = \frac{\rho\,\omega\,R^2}{\eta}, \tag{12}$$

and the functions, K, are modified Bessel Functions. Here, ρ is the density of the fluid and η is its viscosity while $\omega = 2\pi f$.

The function on the right-hand side of Eq. (1) is now fully defined, and it is the mathematical expression used to obtain an optimum fit to the measured resonance curve and thereby to determine the viscosity of the fluid when everything else is known.

The density of the fluid is determined from the resonant frequency of the wire immersed in the fluid at the experimental temperature using the equation,

$$f_0^2 = f_{0,\mathrm{vac}}^2 - \frac{\rho\,g\,V_\mathrm{W}}{16\pi\,L^2\rho_\mathrm{s}R^2}, \tag{13}$$

in which g is the acceleration due to gravity and V_W is the volume of the weight suspended from the wire. The symbol $f_{0,\mathrm{vac}}$ represents the resonant frequency of the wire at the same temperature in vacuo. Thus, the density of the fluid may be evaluated from the same resonance measurements that yield the viscosity if the necessary characteristics of the vibrating-wire assembly are known.

The characteristics of the vibrating-wire assembly may be determined by either direct measurement or by calibration. Table II lists the various characteristics of the assembly together with the method employed for their measurement and the results. The determination of the radius of the

Table II. Characteristic Parameters of Vibrating-Wire Viscometer

Parameter	Measurement method	Value
$f_{0,\mathrm{vac}}$	From the resonance curve in vacuo at 348.35 K	1221.27 Hz
Δ_0	From the resonance curve in vacuo at 348.35 K	66×10^{-6}
L	Direct measurement with a cathetometer; at 273.15 K	36.434 mm
ρ_s	Literature [6]	19,300 kg·m^{-3}
R	Calibration in *n*-decane at 348.35 K and 0.1 MPa	49.953 μm
V_w	Calibration in *n*-decane at 348.35 K and 0.1 MPa	77.080×10^{-6} m^3

wire, R, and the volume of the suspended weight, V_W, were most accurately performed by calibration in n-decane for which the viscosity and density are known from the work of Dymond and Oye [7] and the density from the work of Assael et al. [8]. Changes to the dimensions of the wire and the suspended weight under temperature and pressure changes were evaluated using the relevant coefficients of linear expansion and compressibility [6].

The uncertainty of measurements made with this viscometer has been subject to careful analysis [4] for measurements on pure fluids and mixtures that are well characterized and of repeatable and stable composition. In such cases it is estimated that the uncertainty in both density and viscosity measurement is approximately ±1%. However, in the case of mixtures of the type studied here that contain volatile components and dissolved gases the repeatability of the measurements was significantly worse than is implied by this uncertainty. This lack of repeatability is attributed to variations in the composition between different samples of nominally the same material. For that reason it is estimated that the uncertainty of the viscosity data reported here is ±5% while it is ±2% for the density data.

3. RESULTS

The viscosity and density of Dutrex were successfully measured along isotherms at $T = 399.13, 423.95, 449.56, 472.70, 497.19, 522.61$, and 546.07 K. No reaction was observed with this hydrocarbon over this temperature range. The fluid was found to contain components that are relatively volatile. As a result, all the measurements for Dutrex were performed with a higher starting pressure of about 1.5 MPa. The measured viscosity and density of Dutrex are presented in Table III. Both these properties of Dutrex increase linearly with increasing pressure at constant temperature, and decrease with increasing temperature.

The mass fraction of hydrogen gas in Dutrex/H_2 Mix 1 was 1.24×10^{-3} and that of Dutrex/H_2 Mix 2 was 5.36×10^{-4}. However, this small quantity was sufficient to enable reactions to take place at temperatures above 473 K, transforming the composition of these mixtures. This compositional change was probably the result of a hydrogenation-type reaction or thermal decomposition. It was deduced from a break in trend of the measurements at the lower temperatures. Therefore, only the results from the four isotherms with the lower temperatures are presented here. Analysis of the viscosity and density of the mixtures in Tables IV and V and of Dutrex in Table III indicates that the dissolved hydrogen makes Dutrex less viscous and less dense at a particular temperature and pressure. The general trend is one where the

Table III. Viscosity and Density of Dutrex as a Function of Temperature and Pressure

P (MPa)	η (mPa·s)	ρ (kg·m^{-3})	P (MPa)	η (mPa·s)	ρ (kg·m^{-3})
	$T=399.13$ K			$T=423.95$ K	
1.38	8.244	994.4	1.43	4.792	976.4
5.21	8.886	997.0	5.09	5.152	979.0
10.24	9.827	999.8	10.09	5.535	983.7
15.03	10.745	1003.1	15.11	6.056	986.8
18.68	11.373	1006.7	19.14	6.458	989.6
14.43	10.453	1003.2	15.06	6.012	987.5
10.03	9.802	1000.0	10.08	5.534	983.8
5.26	8.902	997.7	5.03	5.177	979.2
1.59	8.349	994.1	1.51	4.829	977.1
	$T=449.56$ K			$T=472.70$ K	
1.49	3.108	956.0	1.42	2.247	940.0
5.07	3.270	960.2	5.03	2.357	944.7
10.12	3.525	965.1	10.01	2.541	949.6
15.05	3.778	969.9	15.02	2.749	953.9
19.59	4.065	973.0	19.19	2.904	957.6
15.19	3.811	969.3	15.04	2.736	954.2
10.23	3.547	964.7	10.03	2.572	948.5
5.12	3.280	959.9	5.05	2.369	944.1
1.54	3.110	956.0	1.49	2.250	940.3
	$T=497.19$ K			$T=522.61$ K	
1.44	1.674	922.7	1.91	1.470	902.7
5.20	1.774	926.8	5.11	1.545	907.3
10.10	1.895	932.5	10.10	1.664	912.7
15.13	2.023	938.0	15.07	1.784	917.7
19.12	2.139	942.0	19.16	1.880	924.5
15.07	2.039	937.6	14.74	1.773	916.6
10.07	1.898	932.2	10.01	1.658	911.7
5.11	1.775	926.8	5.07	1.541	907.7
1.44	1.679	922.3	2.17	1.479	903.0
	$T=546.07$ K				
2.04	1.338	885.6			
5.04	1.415	890.0			
10.10	1.525	896.1			
15.09	1.630	903.0			
19.11	1.718	908.4			
14.89	1.627	902.8			
10.01	1.524	896.9			
5.11	1.415	889.7			
2.31	1.351	886.0			

Table IV. Viscosity and Density of Dutrex/H_2 Mix1 ($w = 1.24 \times 10^{-3}$)

P (MPa)	η (mPa · s)	ρ (kg · m^{-3})	P (MPa)	η (mPa · s)	ρ (kg · m^{-3})
	$T = 399.66$ K			$T = 423.12$ K	
19.01	7.979	937.6	18.97	4.880	926.4
16.59	7.627	936.5	16.59	4.679	925.6
14.12	7.287	935.2	14.11	4.468	924.8
16.55	7.588	936.9	16.56	4.646	925.9
19.04	7.964	938.1	19.07	4.848	926.8
	$T = 448.98$ K			$T = 473.36$ K	
19.04	3.252	918.0	14.07	2.199	900.3
16.63	3.150	915.4	16.58	2.255	903.4
14.42	3.055	912.8	19.22	2.335	905.7
16.63	3.131	915.6	16.61	2.259	903.4
19.12	3.256	917.8	14.08	2.199	900.4

Table V. Viscosity and Density of Dutrex/H_2 Mix 2 ($w = 5.36 \times 10^{-4}$)

P (MPa)	η (mPa · s)	ρ (kg · m^{-3})	P (MPa)	η (mPa · s)	ρ (kg · m^{-3})
	$T = 399.49$ K			$T = 424.02$ K	
19.67	9.057	989.0	19.60	5.437	974.7
17.65	8.763	986.9	17.65	5.284	973.3
15.73	8.504	985.0	15.62	5.139	971.5
13.73	8.262	982.9	13.51	4.975	970.0
15.76	8.541	985.0	15.72	5.158	972.3
17.70	8.794	987.0	17.68	5.317	974.0
19.53	9.012	988.9	19.44	5.485	975.0
	$T = 448.63$ K			$T = 471.86$ K	
13.54	3.352	960.0	13.59	2.490	950.5
15.66	3.440	962.8	15.64	2.571	952.4
17.71	3.564	964.2	17.71	2.658	954.0
19.57	3.647	966.5	19.56	2.751	955.5
17.58	3.556	964.8	17.50	2.640	953.7
15.60	3.460	963.2	15.70	2.580	953.0
13.64	3.375	961.6	13.80	2.500	951.0

higher the concentration of hydrogen gas, the lower the viscosity and density of the mixture. Figures are omitted here in the interests of brevity but it emerges that the viscosity and density of the mixtures are linear functions of pressure along an isotherm.

The viscosity and density of ALFD were successfully measured from 399.2 to 546.8 K, along seven isotherms. Like Dutrex, it contains volatile components and so the lowest pressure of measurements employed was about 1.5 MPa. The measured viscosity and density values of ALFD are summarized in Table VI. Comparison of the data in these tables with results for Dutrex shows that ALFD is less viscous and less dense than Dutrex.

Table VI. Viscosity and Density of ALFD

P (MPa)	η (mPa · s)	ρ (kg · m^{-3})	P (MPa)	η (mPa · s)	ρ (kg · m^{-3})
	$T = 399.20$ K			$T = 423.46$ K	
1.88	5.546	901.1	1.47	3.998	880.8
4.89	5.808	903.7	5.05	4.209	883.8
10.12	6.236	908.1	10.05	4.513	888.0
15.12	6.805	912.3	15.11	4.857	892.2
19.19	7.213	915.7	19.14	5.153	895.7
15.13	6.783	913.3	15.08	4.845	892.2
10.07	6.282	908.1	9.97	4.521	887.9
4.94	5.796	903.7	5.04	4.220	883.8
1.89	5.509	901.2	1.45	4.079	880.7
	$T = 448.05$ K			$T = 472.16$ K	
2.07	2.903	859.1	1.44	2.172	843.0
5.11	3.014	862.8	5.02	2.279	846.0
9.98	3.221	867.7	10.08	2.422	850.6
14.96	3.425	873.3	15.18	2.574	855.2
19.18	3.601	877.7	19.17	2.702	859.8
14.94	3.422	873.5	15.17	2.571	856.4
9.81	3.232	867.7	10.04	2.437	850.3
5.10	3.032	863.3	4.98	2.268	845.8
2.05	2.885	860.3	1.47	2.168	842.3
	$T = 498.01$ K			$T = 522.72$ K	
2.02	1.598	821.4	1.42	1.200	797.4
5.05	1.666	824.1	4.95	1.268	801.7
10.11	1.780	828.9	10.17	1.365	809.3
15.10	1.892	833.2	15.15	1.465	815.2
19.44	1.989	839.5	18.08	1.513	818.7
15.01	1.890	832.7	15.02	1.475	814.8
10.07	1.779	828.9	9.92	1.378	808.5
4.97	1.665	824.3	4.98	1.273	802.8
2.0	1.598	821.3	1.48	1.207	797.7
	$T = 546.80$ K				
1.72	0.921	778.2			
5.19	0.971	781.1			
10.17	1.043	785.3			
15.11	1.115	789.5			
19.19	1.166	792.9			
14.95	1.116	789.3			
9.95	1.047	785.1			
4.95	0.959	780.9			
1.71	0.925	778.2			

The amount of hydrogen in the two mixtures of ALFD was of the same order of magnitude as in the corresponding Dutrex/H_2 mixtures. However, in this case the dissolved solute gas did not react with the ALFD over the measured temperature range of 397.7 to 549.1 K. The viscosity and density along all seven isotherms for each mixture are listed in Tables VII and VIII. For ALFD/ H_2 Mix 1 the mass fraction of hydrogen was 1.25×10^{-3} and for ALFD/ H_2 Mix 2 it was 6.33×10^{-4}. Comparisons of the tabulated data for the mixtures and for pure ALFD indicate that the mixtures have lower viscosities and densities than the pure sample at any given

Table VII. Viscosity and Density of ALFD/H_2 Mix 1 ($w = 1.25 \times 10^{-3}$)

P (MPa)	η (mPa · s)	ρ (kg · m^{-3})	P (MPa)	η (mPa · s)	ρ (kg · m^{-3})
	$T = 398.97$ K			$T = 423.86$ K	
12.08	5.993	853.4	11.97	3.968	833.2
14.52	6.124	855.4	14.44	4.075	835.0
17.17	6.408	857.6	17.05	4.204	838.1
19.56	6.671	859.6	19.57	4.344	840.7
17.20	6.471	857.6	16.81	4.199	838.0
14.59	6.178	855.3	14.57	4.089	836.0
12.21	5.971	853.4	12.16	3.954	833.2
	$T = 448.41$ K			$T = 473.26$ K	
12.10	2.844	813.9	12.23	2.041	793.5
14.56	2.948	816.1	14.63	2.102	796.1
16.99	3.023	818.1	17.09	2.159	800.4
19.47	3.106	820.5	19.58	2.213	803.5
16.95	3.020	819.6	17.11	2.157	798.6
14.41	2.930	817.3	14.63	2.088	796.2
12.13	2.830	813.1	12.14	2.041	794.9
	$T = 498.25$ K			$T = 522.84$ K	
12.44	1.584	774.1	12.45	1.189	757.8
14.73	1.614	778.2	14.77	1.218	760.0
17.27	1.645	781.7	17.24	1.244	762.2
19.66	1.680	782.9	19.69	1.265	763.1
17.28	1.640	781.5	17.24	1.241	761.8
14.67	1.613	778.3	14.64	1.218	760.4
12.37	1.583	775.9	12.31	1.184	757.1
	$T = 548.06$ K				
12.25	0.957	735.9			
14.67	0.981	738.8			
17.28	1.006	741.8			
19.69	1.030	744.7			
17.14	1.005	741.7			
14.59	0.980	738.7			
12.31	0.957	736.0			

Table VIII. Viscosity and Density of ALFD/H_2 Mix 2 ($w = 6.33 \times 10^{-4}$)

P (MPa)	η (mPa · s)	ρ (kg · m^{-3})	P (MPa)	η (mPa · s)	ρ (kg · m^{-3})
	$T = 397.68$ K			$T = 423.58$ K	
9.16	6.041	857.1	9.04	3.963	834.9
11.86	6.255	858.7	12.08	4.088	838.4
14.93	6.500	861.1	15.11	4.212	841.4
18.97	6.821	864.1	19.10	4.379	844.7
14.92	6.499	862.0	14.92	4.222	841.0
11.91	6.259	859.7	11.94	4.072	838.3
9.15	6.040	857.2	9.06	3.946	835.4
	$T = 477.86$ K			$T = 472.64$ K	
9.14	2.790	818.2	9.32	2.105	795.7
12.07	2.911	821.0	12.39	2.183	800.0
15.11	3.042	822.9	15.32	2.252	801.7
19.11	3.167	827.0	19.33	2.350	806.9
14.97	3.033	823.4	15.41	2.252	801.8
11.92	2.898	820.6	12.45	2.178	799.9
9.01	2.766	816.9	9.50	2.107	796.9
	$T = 497.90$ K			$T = 522.41$ K	
9.40	1.594	778.7	9.37	1.214	756.9
12.47	1.642	782.1	12.50	1.257	761.0
15.23	1.692	785.2	15.21	1.302	765.1
19.29	1.773	788.7	19.25	1.372	768.0
15.36	1.696	786.2	15.38	1.307	764.7
12.34	1.629	781.0	12.30	1.271	761.2
9.39	1.589	778.7	9.41	1.212	757.0
	$T = 549.10$ K				
9.25	0.974	735.8			
12.37	1.022	740.2			
15.48	1.070	743.6			
19.34	1.130	749.0			
15.28	1.067	743.2			
12.45	1.024	739.1			
9.31	0.975	736.1			

temperature and pressure. ALFD/H_2 Mix 1, which contained the highest concentration of hydrogen gas, was the least viscous and least dense among the three compositions of ALFD studied. Again, the viscosity and density are linear functions of pressure along an isotherm.

4. REPRESENTATION

All of the experimental results have been represented by an equation of the form,

$$\eta = \eta_0 + \eta_1 p, \tag{14}$$

Table IX. Coefficients in the General Empirical Correlations for Each Hydrocarbon/Gas Mixture

Coefficient	Dutrex/H_2	ALFD/H_2
w_1	1.236×10^{-3}	1.244×10^{-3}
b_1	1.146	0.177
b_2	224.03×10^3	1.029×10^3
b_3	0.026	0.013264
b_4	0.021	0.014
b_5	352.6×10^3	8.316×10^3
b_6	0.0315	0.0291
c_1	0.048	0.291
c_2	3.145×10^3	0.949×10^3
c_3	0.0161	0.0137
c_4	0.041	0.011
c_5	6620×10^4	8.208×10^4
c_6	0.0511	0.0338
AAD (%)	1.85	1.8
MAD (%)	5.2	5.0

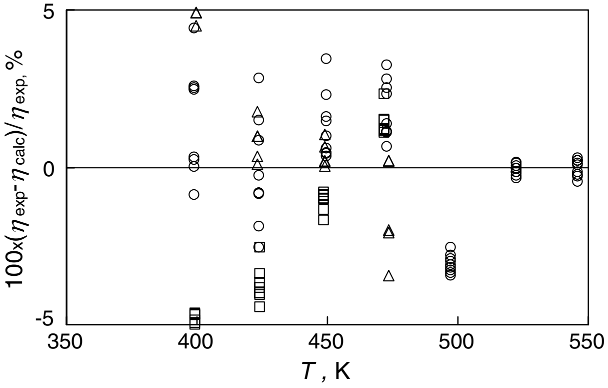

Fig. 4. Deviation of the experimental viscosity of Dutrex and Dutrex/H_2 mixtures from the general correlation. ○ Dutrex; △ Dutrex/H_2 Mix 1; □ Dutrex /H_2 Mix 2.

where the viscosity is in mPa·s and the pressure is in MPa. The coeffcients η_0 and η_1 are dimensionless functions of temperature and hydrogen mass fraction and are given by

$$\eta_0 = b_1 + b_2 \exp(-b_3 T) + (w/w_1)\left[c_1 - b_1 + c_2 \exp(-c_3 T) - b_2 \exp(-b_3 T)\right], \tag{15}$$

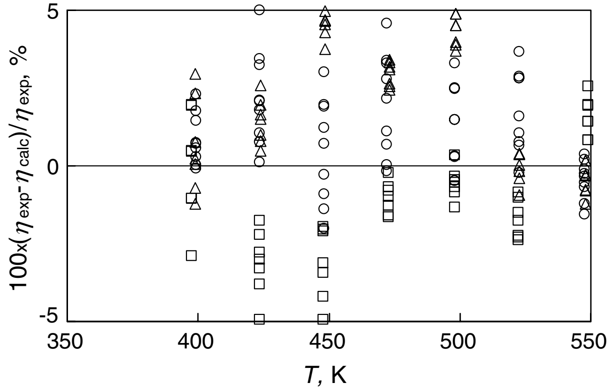

Fig. 5. Deviation of the experimental viscosity of ALFD and ALFD/H_2 mixtures from the general correlation. ○ ALFD; △ ALFD/H_2 Mix 1; □ ALFD/H_2 Mix 2.

and

$$\eta_1 = b_4 + b_5 \exp(-b_6 T) + (w/w_1)\,[c_4 - b_4 + c_5 \exp(-c_6 T) - b_5 \exp(-b_6 T)]\,. \tag{16}$$

The specific form of these correlations is consistent with the following empirical observations: (a) η is a precise linear function of p at constant T and w; (b) η is an approximately linear function of w at constant T and p; and (c) the viscosity obeys an equation of the form $\eta = a + b\exp(-cT)$ at constant p and w. The coefficients of Eqs. (15) and (16) are given in Table IX together with the average absolute deviation (AAD) and the maximum absolute deviation (MAD) for each fluid system studied.

Figure 4 shows deviations of the experimental viscosity data from this correlation for Dutrex/H_2 mixtures whereas Fig. 5 contains the same information for the ALFD/H_2 mixtures. The deviations are generally consistent with the estimated uncertainty of ±5% in these results.

ACKNOWLEDGMENT

This work was sponsored in part by Shell International.

REFERENCES

1. T. Retsina, S. M. Richardson, and W. A. Wakeham, *Appl. Sci. Res.* **43**:127 (1986).
2. T. Retsina, S. M. Richardson, and W. A. Wakeham, *Appl. Sci. Res.* **43**:325 (1986).

3. A. A. H. Padua, J. M. N. A. Fareleira, J. C. G. Calado, and W. A. Wakeham, *Int. J. Thermophys.* **17**:781 (1996).
4. C. W. Len, *Viscosity of Heavy Hydrocarbons with Dissolved Gases*, (Ph. D. Thesis, Imperial College, London, 2003).
5. C. M. B. P. Oliveira and W. A. Wakeham, *Int. J. Thermophys.* **13**:773 (1992).
6. *Metals Handbook*, 8^{th} Ed. (American Society for Metals, New York, 1961), p. 1225.
7. J. H. Dymond and H. A. Oye, *J. Phys. Chem. Ref. Data* **23**:41(1994).
8. M. J. Assael, J. H. Dymond, and D. Exadaktilou, *Int. J. Thermophys.* **15**:155 (1994).